

Network-complement transitions, symmetries, and cluster synchronization

Takashi Nishikawa^{1,2} and Adilson E. Motter^{1,2}

¹*Department of Physics and Astronomy, Northwestern University, Evanston, IL 60208, USA*

²*Northwestern Institute on Complex Systems, Northwestern University, Evanston, IL 60208, USA*

Synchronization in networks of coupled oscillators is known to be largely determined by the spectral and symmetry properties of the interaction network. Here we leverage this relation to study a class of networks for which the threshold coupling strength for global synchronization is the lowest among all networks with the same number of nodes and links. These networks, defined as being uniform, complete, and multi-partite (UCM), appear at each of an infinite sequence of network-complement transitions in a larger class of networks characterized by having near-optimal thresholds for global synchronization. We show that the distinct symmetry structure of the UCM networks, which by design are optimized for global synchronizability, often leads to formation of clusters of synchronous oscillators, and that such states can coexist with the state of global synchronization.

The study of dynamical processes on networks has traditionally been centered on establishing relations between the collective behavior and structures in the network of existing interactions.¹ Here we focus on the role played more explicitly by structures in the complement of the network, which can be interpreted as the network of absent interactions. While the information provided by the network and its complement are mathematically equivalent, the interpretation of the results is easier and more natural in the complement. We focus on the class of networks with minimum possible size of the largest components in their complement (MCC). We show that 1) MCC networks approach those that maximize global synchronizability (i.e., that require the smallest coupling strength for stable synchronization), 2) MCC networks exhibit an infinite sequence of transitions, each defining a UCM network characterized by being strictly optimal, and 3) the dynamics of UCM networks can be rich yet permits systematic identification of stability thresholds. This work shows that the optimization of network structure for synchronization leads to significantly different results and is surprisingly more involved for undirected networks considered here when compared to the previously solved problem of directed networks².

transitions can be “explosive,” which was followed by a surge of investigation on their exact nature,^{6–8} and has highlighted the fact that even single-link modification can have large impact on global structural properties.⁹ An influential example of a dynamical transition is the sudden emergence of a synchronized subpopulation in Kuramoto’s network of globally coupled phase oscillators¹⁰ as the coupling strength increases, which was more recently extended to the case of more complex coupling structures.^{11–14} It has been shown that such synchronization transitions can also be explosive when correlation exists between the natural frequencies of the oscillators and the network structure.^{15,16} Here we consider transitions involving both structure and dynamics: structural transitions in the class of MCC networks, which is defined through the impact their network structure has on a (different) dynamical transition—namely, the stability transition for global synchronization. As the space of MCC networks is traversed by varying the total number of links in the network, structural transitions in the complement of the network is observed at special points that defines the UCM networks.

Optimizing the network structure for dynamics is a widely studied problem in the context of networks and complex systems, particularly in the context of maximizing global synchronizability.^{2,17–23} Recent studies on network synchronization dynamics^{24–26} have also encompassed various other forms of synchronization, such as cluster synchronization,^{27–29} remote synchronization,^{30–32} relay synchronization,³³ and chimera states.^{34,35} Here we show that the UCM networks, despite being designed to optimize global synchronization, often exhibit cluster synchronization. This counter-intuitive effect can be attributed to their highly symmetric structure, which is a byproduct of the optimization that also allows us to develop systematic stability analysis for cluster synchronization.

I. INTRODUCTION

In the study of networks there are two major classes of transitions that can be observed as an external parameter is varied: *structural transitions*, in which a sudden change occurs in the connectivity structure of the network, and *dynamical transitions*, in which the change occurs in the collective behavior of a network of coupled dynamical entities. A primary example of a structural transition is the widely studied problem of network percolation,^{3,4} in which the relative size of the largest connected component of random networks exhibits a phase transition as the average number of links per node increases. It has recently been discovered⁵ that such

II. STABILITY OF GLOBAL SYNCHRONIZATION

The dynamical model we use for a network of coupled oscillators is the Pecora-Carroll model³⁶ with the following no-

tation. The governing equation reads

$$\dot{\mathbf{x}}_i = \mathbf{F}(\mathbf{x}_i) + \varepsilon \sum_{j=1}^n A_{ij} [\mathbf{H}(\mathbf{x}_j) - \mathbf{H}(\mathbf{x}_i)], \quad i = 1, \dots, n. \quad (1)$$

We assume that the dynamics of an isolated oscillator, $\dot{\mathbf{x}}_i = \mathbf{F}(\mathbf{x}_i)$, is chaotic and identical for all oscillators. We also assume that the network encoded by the adjacency matrix $A = (A_{ij})_{1 \leq i, j \leq n}$ is undirected (i.e., $A_{ij} = A_{ji}$), unweighted (i.e., $A_{ij} = 1$), and connected. Using the corresponding Laplacian matrix L , defined by

$$L_{ij} = \begin{cases} -A_{ij} & \text{if } i \neq j, \\ \sum_{k \neq i} A_{ik} & \text{if } i = j, \end{cases} \quad (2)$$

system (1) can be written as

$$\dot{\mathbf{x}}_i = \mathbf{F}(\mathbf{x}_i) - \varepsilon \sum_{j=1}^n L_{ij} \mathbf{H}(\mathbf{x}_j). \quad (3)$$

For any given dynamics of an isolated oscillator $\mathbf{x}_{\text{GS}} = \mathbf{x}_{\text{GS}}(t)$ (satisfying $\dot{\mathbf{x}}_{\text{GS}} = \mathbf{F}(\mathbf{x}_{\text{GS}})$), there is a corresponding solution of Eq. (1) describing a state of *global synchronization* (GS), given by $\mathbf{x}_i(t) = \mathbf{x}_{\text{GS}}(t)$ for all i and all t . The stability of this solution can be analyzed using the master stability function approach³⁶, which is based on the linearization of Eq. (1) around the globally synchronous state and the transformation of the state variables to eigenvector coordinates of the Laplacian matrix L . The result of this analysis is a master stability function (MSF), which is denoted by $\Lambda_{\text{GS}}(\alpha)$ and defined to be the maximum Lyapunov exponent of

$$\delta \dot{\mathbf{x}} = [D\mathbf{F}(\mathbf{x}_{\text{GS}}) - \alpha D\mathbf{H}(\mathbf{x}_{\text{GS}})] \delta \mathbf{x}, \quad (4)$$

where α is an auxiliary parameter. The condition for the stability of the globally synchronous state is

$$\max_{2 \leq j \leq n} \Lambda_{\text{GS}}(\varepsilon \lambda_j) < 0, \quad (5)$$

where $0 = \lambda_1 < \lambda_2 \leq \dots \leq \lambda_n$ are the eigenvalues of L . Note that $\lambda_1 = 0$ because the Laplacian is a zero row sum matrix, λ_j are all real because L is a symmetric matrix for undirected networks, and $\lambda_2 > 0$ because the network is assumed to be connected. Since the oscillators are chaotic, GS is unstable when there is no coupling between them (i.e., when $\varepsilon = 0$), implying $\Lambda_{\text{GS}}(0) > 0$. For any MSF that is negative on a semi-infinite interval (i.e., $\Lambda_{\text{GS}}(\alpha) < 0$ on (α_1, ∞) with $\alpha_1 > 0$), the threshold coupling strength—the minimum value of ε for which GS is stable—is given by $\alpha_1 / \lambda_2 \equiv \varepsilon_1^{\text{th}}$. For an MSF that is negative on a finite interval (α_1, α_2) with $0 < \alpha_1 < \alpha_2$, there can be networks that are not synchronizable at all (i.e., have no value of ε that allows $\alpha_1 < \varepsilon \lambda_2 \leq \varepsilon \lambda_n < \alpha_n$ to be satisfied). In that case, the value $\varepsilon_1^{\text{th}}$ is the coupling threshold for GS for all synchronizable networks. Thus, the larger the value of λ_2 , the lower the threshold for the stability of GS. The eigenvalue λ_2 is also known to be important for other processes, such as diffusion dynamics,^{37,38} consensus protocol,^{39,40} and Turing instability in activator-inhibitor systems.⁴¹

III. NETWORK-COMPLEMENT TRANSITIONS

The problem of identifying and characterizing the networks maximizing λ_2 (and thus minimizing $\varepsilon_1^{\text{th}}$) for a given number of nodes and links is a challenging problem that has been a topic of investigation in the mathematics communities.^{42–45} As we see below, in some cases this problem can be completely solved. Indeed, if $n = k\ell$ with integers k and ℓ and the number of links is $m = \frac{1}{2}k^2\ell(\ell - 1)$, it can be shown that the maximum possible value $\lambda_2 = n - k$ is achieved only by the *UCM network*, defined as the network having ℓ groups of k oscillators (i.e., uniform group size) in which the groups are fully connected to each other (i.e., complete), but have no internal links within any group (i.e., multi-partite). For other combinations of n and m , a class of networks that share a unique property with the UCM networks can be defined and shown⁵³ to have maximal or near-maximal λ_2 values for a wide range of the parameters n and m . We refer to such networks as *MCC networks*, since they are defined to be the networks that have the minimum possible size of the largest components in their graph complement among all networks with the same n and m . Here, *components* of a given network refer to the connected components of the network, and the *complement* of a given network with adjacency matrix A is defined as the network with the adjacency matrix A^c given by $A_{ij}^c = 1$ if $A_{ij} = 0$ with $i \neq j$, $A_{ij}^c = 0$ if $A_{ij} = 1$ with $i \neq j$, and $A_{ii} = 0$. It follows that the UCM networks, whose complement consists of ℓ fully connected components of size k , are special cases of MCC networks.

We now study the structural properties of the complement of the UCM and MCC networks as a function of the number of links. Let $k_n^*(m)$ denote the size of the largest components in the complement of the MCC network with n nodes and m links. This integer-valued function can be expressed as

$$k_n^*(m) = \lceil C_{n,m} \cdot n \rceil, \quad C_{n,m} \equiv \frac{\ell + \sqrt{\ell^2 - \frac{2m}{n^2} \ell(\ell + 1)}}{\ell(\ell + 1)}, \quad (6)$$

where we denote by $\lceil x \rceil$ the smallest integer greater than or equal to x , and we define ℓ to be the (unique) integer satisfying $m_{\ell,n}^* \leq m < m_{\ell+1,n}^*$ with $m_{\ell,n}^* \equiv \frac{n^2(\ell-1)}{2\ell}$. As m increases from $m = n - 1$ (minimum required for a connected network) to $m = \frac{1}{2}n(n - 1)$ (complete graph) while keeping n fixed, function $k_n^*(m)$ decreases from n to 1, jumping down by one at various points, which are non-uniformly distributed over the range of m values. These jumps are associated with the addition of a link (i.e., deletion of a link in the complement) that for the first time allows for a smaller component size in the complement through global rearrangement of the links (see Fig. 1 for examples). Note that some jumps occur when the network becomes UCM (e.g., at $m = 300$ in Fig. 1, right column), while others occur without the appearance of a UCM network (e.g., at $m = 297$ in Fig. 1, left column).

In order to consider the limit of large network size, we normalize the maximum component size in the complement, $k_n^*(m)$, by its upper bound, n , and express it as a function of the link density, $\phi \equiv \frac{2m}{n(n-1)}$, to obtain the relative compo-

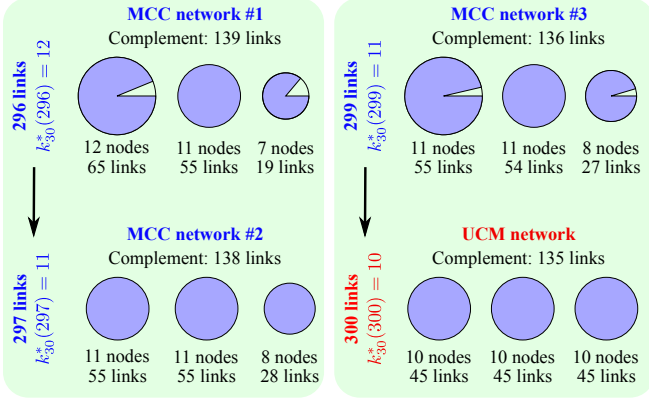


FIG. 1. Examples of network-complement transitions for MCC networks. For each network we visualize its complement, using circles to indicate the connected components and the shaded area to indicate the density of links in these components. (Left) After a single link is added to MCC network #1, it becomes possible to rearrange links to decrease the largest component size in the complement, $k_n^*(m)$, and obtain MCC network #2. (Right) By adding a link to MCC network #3, it also becomes possible to rearrange links not only to decrease $k_n^*(m)$, but also to obtain a UCM network in this case.

nent size $\overline{k}_n^*(\phi) \equiv \frac{1}{n}k_n^*(\frac{1}{2}\phi n(n-1))$. Figure 2(a) shows an example of $\overline{k}_n^*(\phi)$ for MCC networks of size $n = 30$. We observe that $\overline{k}_n^*(\frac{2}{n}) = 1$ and $\overline{k}_n^*(1) = \frac{1}{n}$, with the jumps of size $\frac{1}{n}$ at $n-1$ intermediate points. Defining $\phi_{\ell,n}^* \equiv \frac{2m_{\ell,n}^*}{n(n-1)}$ and taking the limit $m, n \rightarrow \infty$ with fixed ϕ in Eq. (6), we obtain

$$\overline{k}_\infty^*(\phi) = \frac{\ell + \sqrt{\ell^2 - \phi\ell(\ell+1)}}{\ell(\ell+1)}, \quad (7)$$

where ℓ is the (unique) integer satisfying $\phi_{\ell,\infty}^* \leq \phi < \phi_{\ell+1,\infty}^*$ with $\phi_{\ell,\infty}^* \equiv \lim_{n \rightarrow \infty} \phi_{\ell,n}^* = \frac{\ell-1}{\ell}$. The function $\overline{k}_\infty^*(\phi)$ given by Eq. (7) and shown in Fig. 2(b) has an infinite number of non-differentiable points at $\phi_{\ell,\infty}^*$, $\ell = 2, 3, \dots$. Note that the integer ℓ can be interpreted as the number of connected components in the complement in the large-network limit. The transition points $\phi_{\ell,\infty}^*$, at which ℓ makes discrete jumps, correspond to UCM networks with ℓ groups of equal size. Details of the proofs and derivations on the properties of the MCC and UCM networks can be found in Ref. 53.

IV. PATTERNS OF CLUSTER SYNCHRONIZATION

We now go beyond the GS stability threshold $\varepsilon_1^{\text{th}}$ and study the emergence of synchronization patterns in the UCM networks. These networks are optimized for GS, and we now study their partial synchronization properties. As we show next, the group structure of the UCM network allows us to carry out the stability analysis explicitly for cluster synchronization. To reflect this group structure, let us re-index the nodes and denote the state vector for the i -th node in the h -th group by $\mathbf{x}_i^{(h)}$. Using this notation and exploiting the group

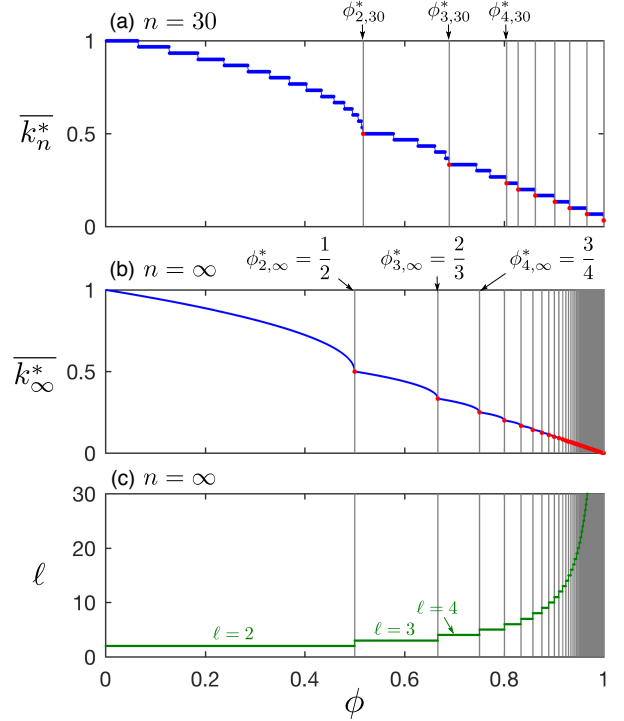


FIG. 2. Infinite sequence of transitions in the complement of MCC networks. (a) Relative size of the largest connected components \overline{k}_n^* in the complement of MCC networks with $n = 30$ nodes as a function of link density ϕ . Vertical lines and red dots indicate the points $\phi = \phi_{\ell,30}^*$, where \overline{k}_n^* jumps down by one. (b) \overline{k}_∞^* given by Eq. (7) for the limit of large networks, $n \rightarrow \infty$. (c) ℓ in the limit $n \rightarrow \infty$, which can be interpreted as the number of components in the complement. The infinite sequence of non-differentiable points of \overline{k}_∞^* (vertical lines and red dots in (b)) indicates the transitions at $\phi = \phi_{\ell,\infty}^*$, $\ell = 2, 3, \dots$, each of which is accompanied by a discrete change in ℓ shown in (c).

structure of the UCM networks, Eq. (3) becomes

$$\dot{\mathbf{x}}_i^{(h)} = \mathbf{F}(\mathbf{x}_i^{(h)}) - \varepsilon k(\ell-1)\mathbf{H}(\mathbf{x}_i^{(h)}) + \varepsilon \sum_{\substack{h'=1 \\ h' \neq h}}^{\ell} \sum_{j=1}^k \mathbf{H}(\mathbf{x}_j^{(h')}). \quad (8)$$

Now consider a state of *cluster synchronization* (CS) given by $\mathbf{x}_i^{(h)}(t) = \mathbf{x}_{\text{CS}}^{(h)}(t)$ for all $i = 1, \dots, k$ and $h = 1, \dots, \ell$. Substituting this into Eq. (8), we obtain an equation of the same form as Eq. (8) but for the network of ℓ nodes, each representing a group of k (synchronized) oscillators:

$$\dot{\mathbf{x}}_{\text{CS}}^{(h)} = \mathbf{F}(\mathbf{x}_{\text{CS}}^{(h)}) - \varepsilon k \sum_{h'=1}^{\ell} \tilde{L}_{hh'} \mathbf{H}(\mathbf{x}_{\text{CS}}^{(h')}), \quad (9)$$

where $\tilde{L} = (\tilde{L}_{hh'})_{1 \leq h, h' \leq \ell}$ is the Laplacian matrix of the fully connected network with ℓ nodes. This is the equation that must be satisfied by the CS state. The special case, $\mathbf{x}_{\text{CS}}^{(h)} = \mathbf{x}_{\text{GS}}(t)$ for all h , which satisfies Eq. (9), describes the synchronization between the groups (in addition to the syn-

chronization of oscillators within each group) and thus corresponds to the globally synchronous state discussed in Sec. II. We can apply the same MSF analysis, since Eq. (9) is just a slight modification of Eq. (3); we obtain Eq. (9) from Eq. (3) by replacing ε with εk and redefining $\tilde{L}_{hh'}$ to represent the all-to-all coupling structure. It follows that the synchronization between the groups is determined by $\Lambda_{\text{GS}}(\varepsilon k \ell) = \Lambda_{\text{GS}}(\varepsilon n)$, since the only nontrivial Laplacian eigenvalue of the size- ℓ fully connected network is ℓ . The Laplacian eigenvalues of a UCM network can be calculated and are 0 , $n - k$, and n , with multiplicity 1 , $\ell(k - 1)$, and $\ell - 1$, respectively. Among these the eigenvalue n corresponds to $\Lambda_{\text{GS}}(\varepsilon n)$, thus associating this eigenvalue with the modes of perturbation that can destroy GS, but not the synchronization within each group.

To analyze the synchronization stability of individual groups, we linearize Eq. (8) around the CS state, which leads to the following variational equation:

$$\delta \dot{\mathbf{x}}_i^{(h)} = [D\mathbf{F}(\mathbf{x}_{\text{CS}}^{(h)}) - \varepsilon k(\ell - 1)D\mathbf{H}(\mathbf{x}_{\text{CS}}^{(h)})]\delta \mathbf{x}_i^{(h)} - \varepsilon \sum_{\substack{h'=1 \\ h' \neq h}}^{\ell} D\mathbf{H}(\mathbf{x}_{\text{CS}}^{(h')}) \sum_{j=1}^k \delta \mathbf{x}_j^{(h')}. \quad (10)$$

If we define $S^{(h)} \equiv \sum_{j=1}^k \delta \mathbf{x}_j^{(h)}$ and sum Eq. (10) over i , we obtain

$$\dot{S}^{(h)} = [D\mathbf{F}(\mathbf{x}_{\text{CS}}^{(h)}) - \varepsilon k(\ell - 1)D\mathbf{H}(\mathbf{x}_{\text{CS}}^{(h')})]S^{(h)} - \varepsilon \sum_{\substack{h'=1 \\ h' \neq h}}^{\ell} D\mathbf{H}(\mathbf{x}_{\text{CS}}^{(h')})S^{(h')}. \quad (11)$$

Now consider those perturbations that do not affect the synchronization of any group, i.e., those for which $S^{(h)}(0) = \sum_{j=1}^k \delta \mathbf{x}_j^{(h)}(0) = 0$ for all h and all i . From Eq. (11), we see that $S^{(h)}(t) = \sum_{j=1}^k \delta \mathbf{x}_j^{(h)}$ remains zero at all times, and hence that the second term in Eq. (10) vanishes. This collapses the k equations for group h into a single equation:

$$\delta \dot{\mathbf{x}}^{(h)} = [D\mathbf{F}(\mathbf{x}_{\text{CS}}^{(h)}) - \varepsilon k(\ell - 1)D\mathbf{H}(\mathbf{x}_{\text{CS}}^{(h)})]\delta \mathbf{x}^{(h)}. \quad (12)$$

Thus, the stability against all perturbations that affect the synchronization of group h is determined by the same equation, while this stability can be different for different groups through the dependence of Eq. (12) on $\mathbf{x}_{\text{CS}}^{(h)}$. The lack of dependence on $h' \neq h$ (i.e., on the states of other groups) in Eq. (12) indicates that we have completely decoupled the problem of synchronization stability for individual groups. Altogether, we have shown that the stability of CS can be analyzed by (i) solving the system of ℓ coupled oscillators in Eq. (9) to obtain $\mathbf{x}_{\text{CS}}^{(h)}$, and then (ii) solving Eq. (12) for each $h = 1, \dots, \ell$. We remark that the result above can also be derived using a general method based on the irreducible representations of the symmetry group²⁹. Here, we were able to derive the results in a simpler and clearer fashion by explicitly using the special structure of the UCM networks, namely the groups with identical size and connectivity patterns. This,

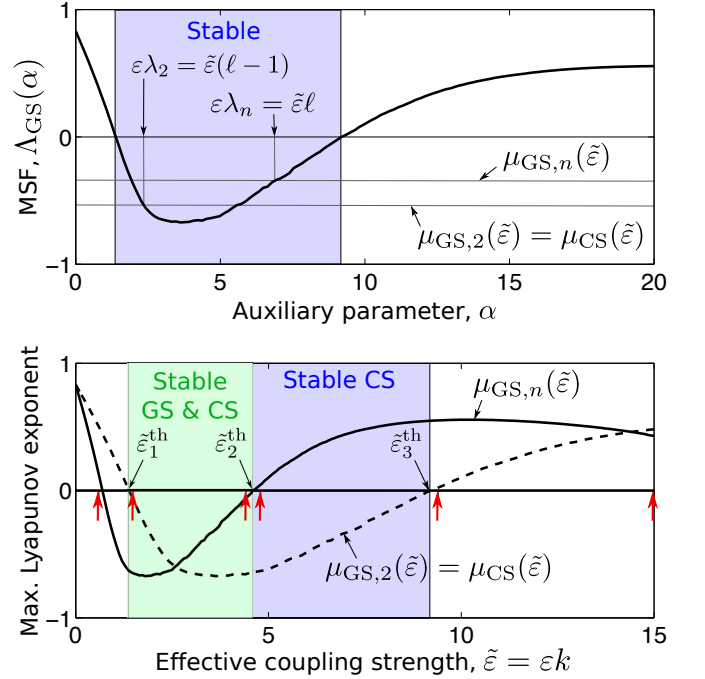


FIG. 3. Stability condition for GS and CS states in UCM networks of coupled Lorenz oscillators with $\ell = 2$ groups of arbitrary size k . (a) MSF as a function of the auxiliary parameter α . The condition for the GS state to be stable is to have both $\varepsilon\lambda_2$ and $\varepsilon\lambda_n$ in the blue-shaded region. (b) The Lyapunov exponents $\mu_{\text{GS},2}(\tilde{\varepsilon}) = \mu_{\text{CS}}(\tilde{\varepsilon})$ and $\mu_{\text{GS},n}(\tilde{\varepsilon})$ plotted as a function of the effective coupling strength $\tilde{\varepsilon}$. The red arrows indicate the values of $\tilde{\varepsilon}$ used in the full-network simulations shown in Figs. 4–6.

however, suggests that there may be other classes of networks for which a similar simplification of the stability analysis is possible (i.e., an equation similar to Eq. (12) can be derived). While determining and classifying all possible CS solutions and their stability from the network's symmetry group is challenging, there have been a number of studies tackling this problem by focusing on specific classes of networks or on specific aspects of the problem^{29,46–52}.

As an example, we consider a network of coupled Lorenz oscillators governed by Eq. (1) with

$$\mathbf{F}(\mathbf{x}) = \begin{pmatrix} \sigma(y - x) \\ x(\rho - z) - y \\ xy - \beta z \end{pmatrix}, \quad \mathbf{H}(\mathbf{x}) = \begin{pmatrix} 0 \\ 0 \\ z \end{pmatrix}, \quad \mathbf{x} = \begin{pmatrix} x \\ y \\ z \end{pmatrix}, \quad (13)$$

and the standard parameter values, $\sigma = 10$, $\rho = 28$, and $\beta = 2$, for which an isolated oscillator is chaotic.⁵⁴ Our choice of $\mathbf{H}(\mathbf{x})$ represents the coupling among the oscillators through their z -components. In terms of x -, y -, and z -components, Eq. (3) reads

$$\begin{aligned} \dot{x}_i &= \sigma(y_i - x_i), \\ \dot{y}_i &= x_i(\rho - z_i) - y_i, \\ \dot{z}_i &= x_i y_i - \beta z_i - \varepsilon \sum_{j=1}^n L_{ij} z_j. \end{aligned} \quad (14)$$

Note that this coupled system has a unique symmetry: it is invariant under the transformation $\{x_i \rightarrow -x_i, y_i \rightarrow -y_i\}$ for any given i . This is due to the symmetry of the individual Lorenz system about the z -axis in phase space, combined with the diffusive nature of the coupling (and thus the invariance holds for an arbitrary network structure). Because of the symmetry, there are 2^{n-1} distinct anti-phase synchronous states of the system, each of which can be encoded by a length- n binary sequence $a = (a_1, a_2, \dots, a_n)$ with $a_i = \pm 1$. (The number of distinct states is 2^{n-1} rather than 2^n because the two sequences related by the flipping of the sign of all a_i both correspond to the same state.) To construct these states, let $\mathbf{x}_{\text{GS}} = \mathbf{x}_{\text{GS}}(t) = (x_{\text{GS}}(t), y_{\text{GS}}(t), z_{\text{GS}}(t))^T$ be the chaotic trajectory of the isolated oscillator (thus satisfying $\dot{\mathbf{x}}_{\text{GS}} = \mathbf{F}(\mathbf{x}_{\text{GS}})$). For each binary pattern a , the state given by $x_i(t) = a_i x_{\text{GS}}(t)$, $y_i(t) = a_i y_{\text{GS}}(t)$, $z_i(t) = z_{\text{GS}}(t)$ for each i can be readily checked to be a valid solution of Eq. (14). Thus, these states, including the globally synchronous state and the cluster synchronous states of UCM networks, are guaranteed to exist, but their stability depends on the network structure and the coupling strength.

Using the analysis from Sec. II, the stability of GS for the coupled Lorenz systems in Eq. (14) is determined by $\Lambda_{\text{GS}}(\alpha)$, which is shown in Fig. 3(a) and is negative on the finite interval (α_1, α_2) , where $\alpha_1 \approx 1.39$ and $\alpha_2 \approx 9.20$. Since the Laplacian eigenvalues of a UCM network are $0, k(\ell - 1)$, and $k\ell$, the stability condition is that both $\mu_{\text{GS},2}(\tilde{\varepsilon}) \equiv \Lambda_{\text{GS}}(\varepsilon k(\ell - 1)) < 0$ and $\mu_{\text{GS},n}(\tilde{\varepsilon}) \equiv \Lambda_{\text{GS}}(\varepsilon k\ell) < 0$ hold. Figure 3(a) illustrates this situation. Note that we have defined the effective coupling strength $\tilde{\varepsilon} \equiv \varepsilon k$, that the quantities $\mu_{\text{GS},2}(\tilde{\varepsilon})$ and $\mu_{\text{GS},n}(\tilde{\varepsilon})$ are functions of $\tilde{\varepsilon}$ for a given ℓ , and hence that the stability condition depends on k only through $\tilde{\varepsilon}$. Thus, the stability of GS is lost when $\mu_{\text{GS},2}(\tilde{\varepsilon}) = 0$ at $\tilde{\varepsilon} = \tilde{\varepsilon}_1^{\text{th}} \equiv \frac{\alpha_1}{\ell - 1}$. Since the function $\Lambda_{\text{GS}}(\alpha)$ has a second zero crossing, there is a second threshold, $\tilde{\varepsilon}_2^{\text{th}} \equiv \frac{\alpha_2}{\ell}$, at which $\mu_{\text{GS},n}(\tilde{\varepsilon}) = 0$. This is when the GS state loses stability. We note that, if the MSF were negative on an semi-infinite interval, such loss of GS stability would not occur.

We now consider the cluster synchronous states of UCM networks. First we note that a subset of the 2^n symmetry-based anti-phase synchronous states reflect the group structure of UCM networks and correspond to CS, whose stability we analyzed above. We can see this in Eq. (9), which for Lorenz oscillators reads

$$\begin{aligned} \dot{x}_{\text{CS}}^{(h)} &= \sigma(y_{\text{CS}}^{(h)} - x_{\text{CS}}^{(h)}), \\ \dot{y}_{\text{CS}}^{(h)} &= x_{\text{CS}}^{(h)}(\rho - z_{\text{CS}}^{(h)}) - y_{\text{CS}}^{(h)}, \\ \dot{z}_{\text{CS}}^{(h)} &= x_{\text{CS}}^{(h)}y_{\text{CS}}^{(h)} - \beta z_{\text{CS}}^{(h)} - \varepsilon \sum_{h'=1}^{\ell} \tilde{L}_{hh'} z_{\text{CS}}^{(h')}. \end{aligned} \quad (15)$$

For each binary pattern a of length ℓ , the state given by $x_{\text{CS}}^{(h)}(t) = a_h x_{\text{GS}}(t)$, $y_{\text{CS}}^{(h)}(t) = a_h y_{\text{GS}}(t)$, and $z_{\text{CS}}^{(h)}(t) = z_{\text{GS}}(t)$ for each h gives a cluster synchronous state. There are $2^{\ell-1}$ distinct states of this type. Again, due to the symmetry, it can be shown for all h that Eq. (12) becomes identical to Eq. (4) with $\alpha = \varepsilon k(\ell - 1)$, collapsing ℓ equations into one. Thus, the stability condition for all these states is

$\mu_{\text{CS}}(\tilde{\varepsilon}) \equiv \Lambda_{\text{GS}}(\varepsilon k(\ell - 1)) = \mu_{\text{GS},2}(\tilde{\varepsilon}) < 0$. Thus, for the system in Eq. (14) the CS states become stable at $\tilde{\varepsilon}_1^{\text{th}}$, which is identical to the stability threshold for the GS state.

Consider for simplicity the case of $\ell = 2$, for which there are only two patterns: $a = (1, 1)$ (corresponding to GS) and $a = (1, -1)$ (corresponding to anti-phase CS). The functions $\mu_{\text{GS},2}(\tilde{\varepsilon}) = \mu_{\text{CS}}(\tilde{\varepsilon})$ and $\mu_{\text{GS},n}(\tilde{\varepsilon})$ are shown in Fig. 3. Figure 4 shows the simulated dynamics of the full network for various values of $\tilde{\varepsilon}$ with $k = 10$. Below the first threshold $\tilde{\varepsilon}_1^{\text{th}} \approx 1.39$, both the globally synchronous state and the cluster synchronous state are unstable, resulting in near-zero correlation between all pairs of oscillators (Fig. 4(a)). Above $\tilde{\varepsilon}_1^{\text{th}}$, we observe bi-stability: both types of synchronous states coexist and are stable (Fig. 4(b)). At $\tilde{\varepsilon}_2^{\text{th}} \approx 4.60$, where $\Lambda_{\text{GS}}(\varepsilon k\ell) = 0$, GS loses its stability. Increasing $\tilde{\varepsilon}$ further, we observe that the CS state become unstable at $\tilde{\varepsilon}_3^{\text{th}} \approx 9.20$, where $\Lambda_{\text{GS}}(\varepsilon k(\ell - 1)) = 0$.

Although this linear stability transition scenario is clear and simple, the actual dynamics of the network is more subtle and rich. Toward the end of the bi-stability regime $\tilde{\varepsilon}_1^{\text{th}} < \tilde{\varepsilon} < \tilde{\varepsilon}_2^{\text{th}}$, trajectories appear to hop back and forth between the GS and CS states, regardless of whether they are initialized near GS or CS state, which is reminiscent of riddled basins.^{55,56} This is illustrated in Fig. 5(a), which shows an example trajectory initialized near a GS state that subsequently approach a CS state and then a GS state (top panels), as well as one initialized near a CS state that approach a GS state and then a CS state (bottom panels). Evidence of riddled basins has been reported for coupled Rössler systems in Ref. 25. Beyond $\tilde{\varepsilon}_2^{\text{th}}$, we observe similar behavior, despite the absence of stable GS state (Fig. 5(b), top panels). This can be interpreted as chaotic intermittent bursts from the CS state. After the CS state loses its stability at $\tilde{\varepsilon}_3^{\text{th}}$, we observe a CS state that is not quite the anti-phase CS state, in which the dynamics of different clusters are not perfectly anti-correlated (Fig. 6(a)). Increasing $\tilde{\varepsilon}$ further, we find a very different state (Fig. 6(b)), in which neither of the two groups defined by the structure of the UCM network are synchronized. The correlation matrix in Fig. 6(b) shows a more complex pattern of synchrony, in which some oscillators are anti-phase synchronized ($C_{ij} \approx -1$) and others are not synchronized at all (C_{ij} closer to 0).

V. CONCLUSIONS

The symmetry of a system has profound impact on its dynamical behavior.⁵⁷ This is particularly insightful for networked systems, for which characterizing the relation between the network structure and dynamics is nontrivial. Our results show that the significant role played by network symmetry for CS stability²⁹ can be exploited to provide systematic analysis of systems with strong network-structural symmetry, such as the UCM networks. Yet, our numerics suggests that bifurcations involving the GS and CS states have much more depth than is expected from the MSF-based stability analysis. A complete characterization of the basins of attraction of these states in the high-dimensional phase space is generally a challenging problem, and our simulation results offer a

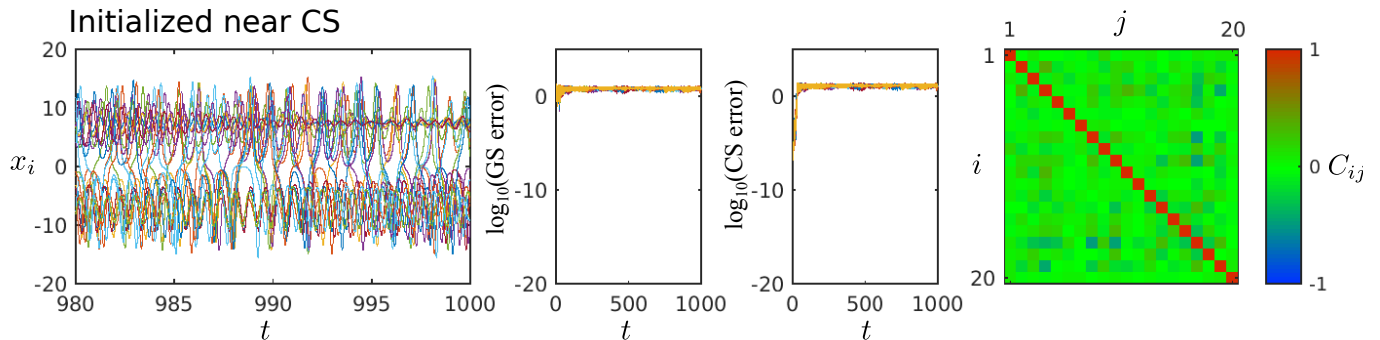
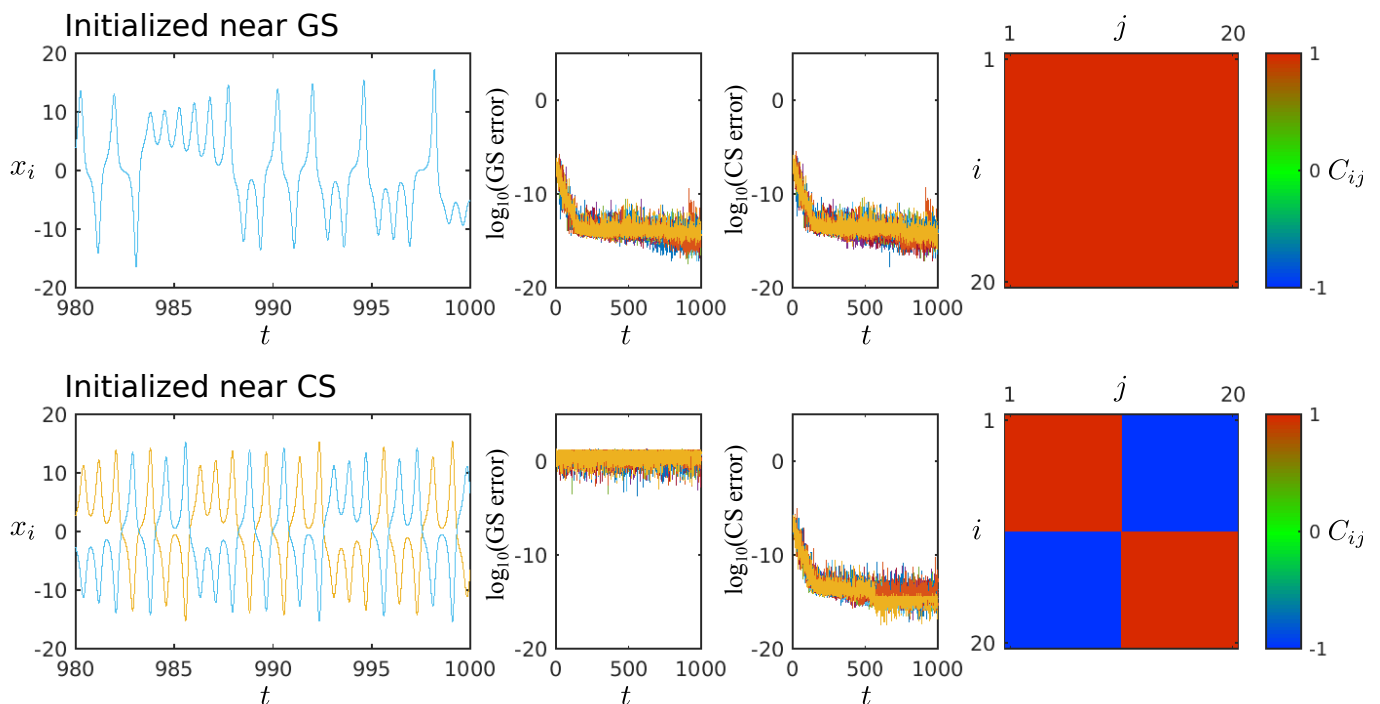
(a) No synchronization: $\tilde{\varepsilon} = 0.6$ (b) Bistability: $\tilde{\varepsilon} = 1.5$ 

FIG. 4. Synchronization dynamics in UCM networks of coupled Lorenz oscillators with $\ell = 2$ groups of size $k = 10$ for various effective coupling strength $\tilde{\varepsilon}$. (a) Ten independent simulations of the full network for $\tilde{\varepsilon} = 0.6$, each initialized at a distance of 10^{-6} from the anti-phase CS state. (b) Simulation results for $\tilde{\varepsilon} = 1.5$. In each row, the leftmost plot shows the x -component of all oscillators, $i = 1, \dots, k\ell = 20$, for a single trajectory initialized as indicated. The next two plots show the synchronization error measured by the standard deviation of x_i over all i for GS and the sum of within-group standard deviations for CS. Ten separate trajectories are shown. The last plot shows the matrix $C = (C_{ij})$, where C_{ij} is the Pearson correlation coefficient of the x -component of oscillator i and j over $500 \leq t \leq 1000$.

glimpse of the rich structure it appears to have. Another possible extension of our work is to consider a variety of other possible patterns of cluster synchronization, which can arise from properties of the system other than network symmetry, such as the internal symmetry of the node dynamics⁴⁶ and the Laplacian property of the coupling matrix⁵².

The fact that network optimization leads to highly symmetric structure in UCM networks suggests a general principle that optimization tends to generate symmetry in networks. While noise, delays, and imperfections may prevent exact symmetries in real systems (or real implementation of

such optimal networks), we expect an elevated level of symmetry in networks under pressure to optimize their function, and there is indeed evidence for abundance of symmetry in real networks.⁵⁸ We suggest that identifying mechanisms by which optimization induces symmetry structures will improve our understanding of the structure-dynamics relation in networks; moreover, it will help design systems with optimized functionality.

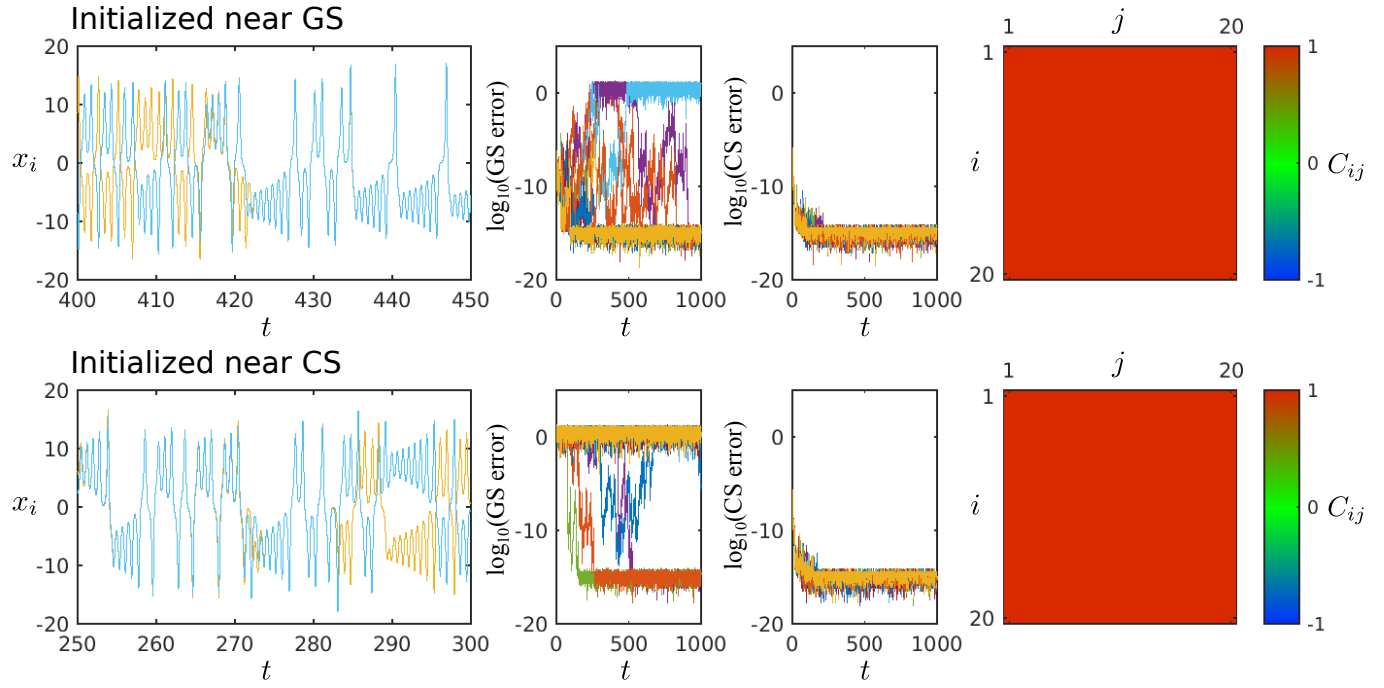
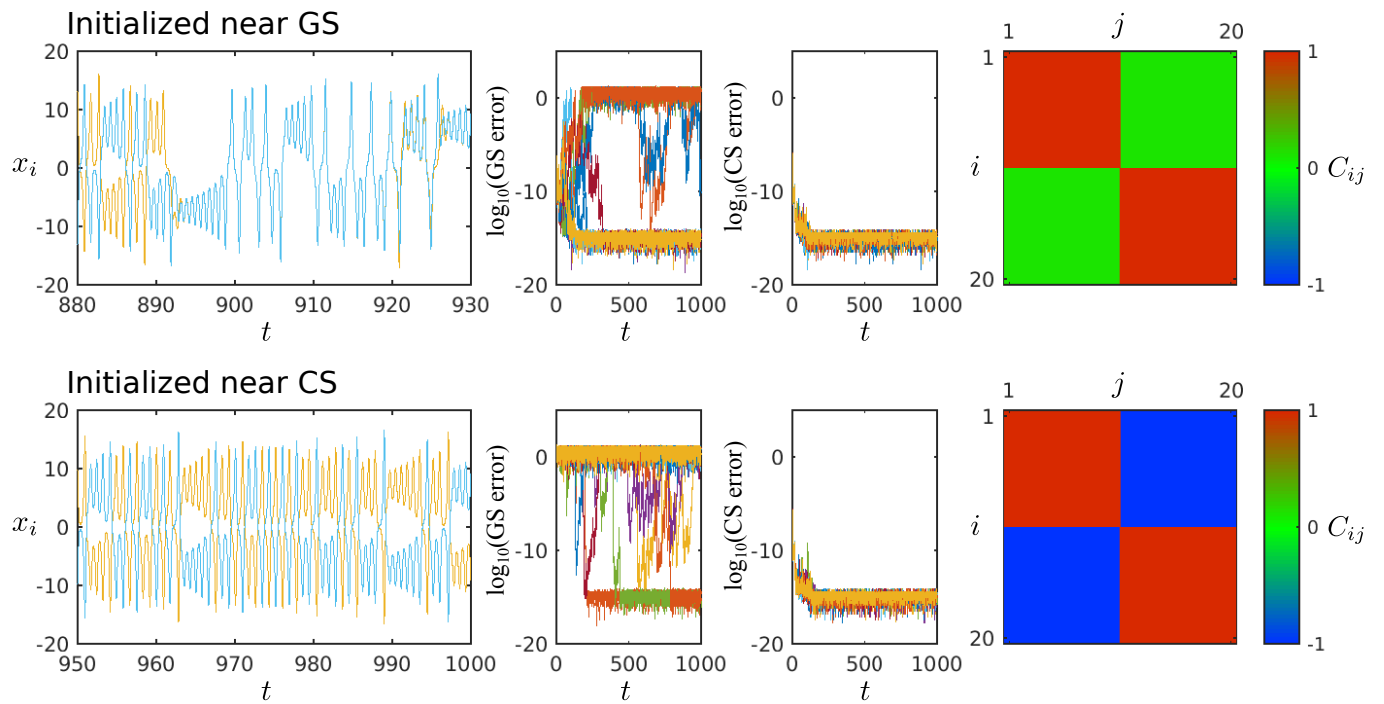
(a) Bistability: $\tilde{\varepsilon} = 4.4$ (b) Unstable GS, stable CS: $\tilde{\varepsilon} = 4.8$ 

FIG. 5. Synchronization dynamics in UCM networks of coupled Lorenz oscillators with $\ell = 2$ groups of size $k = 10$ for $\tilde{\varepsilon} = 4.4$ and $\tilde{\varepsilon} = 4.8$. Detail description of individual plots is the same as in Fig. 4.

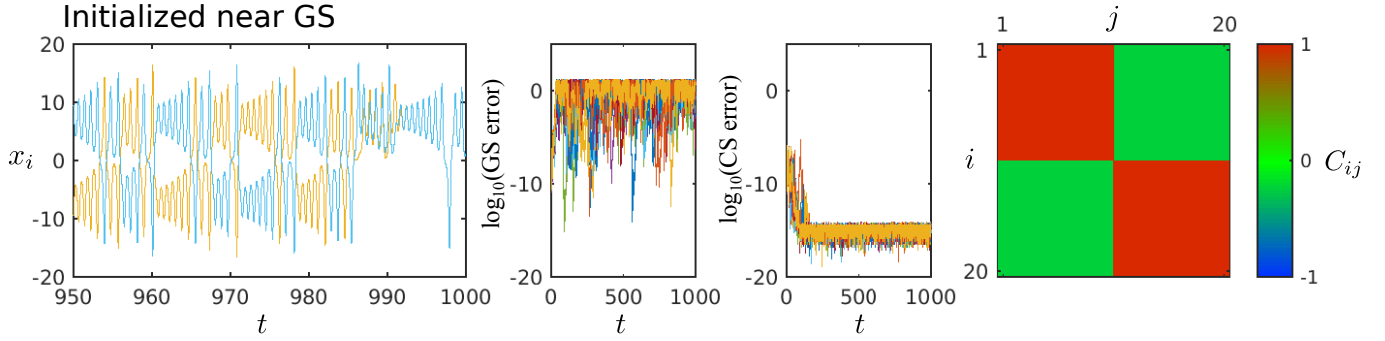
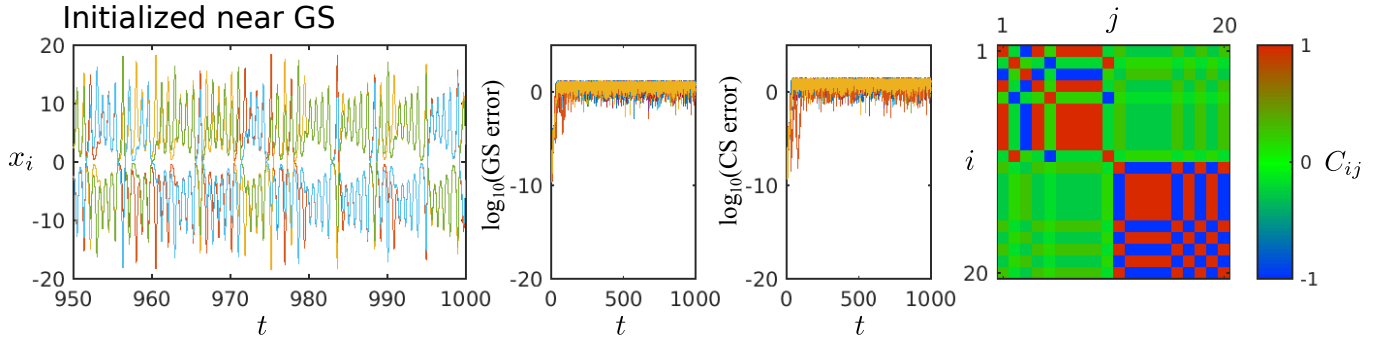
(a) CS but not anti-phase CS: $\tilde{\varepsilon} = 9.4$ (b) More complex CS: $\tilde{\varepsilon} = 15$ 

FIG. 6. Synchronization dynamics in UCM networks of coupled Lorenz oscillators with $\ell = 2$ groups of size $k = 10$ for $\tilde{\varepsilon} = 9.4$ and $\tilde{\varepsilon} = 15$. Detail description of individual plots is the same as in Fig. 4.

ACKNOWLEDGMENTS

The authors thank J. Lehnert and Y. S. Cho for insights on stability analysis for cluster synchronous states, as well as Y. Zhang for valuable discussion on symmetry in synchronization-optimal networks. This work was supported by ARO Grant No. W911NF-15-1-0272.

- ¹M. A. Porter and J. P. Gleeson, *Dynamical Systems on Networks* (Springer, 2016).
- ²T. Nishikawa and A. E. Motter, “Network synchronization landscape reveals compensatory structures, quantization, and the positive effect of negative interactions,” *Proc. Natl. Acad. Sci. U.S.A.* **107**, 10342–10347 (2010).
- ³A. Barrat, M. Barthélemy, and A. Vespignani, *Dynamical Processes on Complex Networks* (Cambridge University Press, 2008).
- ⁴S. N. Dorogovtsev, A. V. Goltsev, and J. F. F. Mendes, “Critical phenomena in complex networks,” *Rev. Mod. Phys.* **80**, 1275 (2008).
- ⁵D. Achlioptas, R. M. D’Souza, and J. Spencer, “Explosive percolation in random networks,” *Science* **323**, 1453–1455 (2009).
- ⁶R. A. da Costa, S. N. Dorogovtsev, A. V. Goltsev, and J. F. F. Mendes, “Explosive percolation transition is actually continuous,” *Phys. Rev. Lett.* **105**, 255701 (2010).
- ⁷O. Riordan and L. Warnke, “Explosive percolation is continuous,” *Science* **333**, 322–324 (2011).
- ⁸R. M. D’Souza and J. Nagler, “Anomalous critical and supercritical phenomena in explosive percolation,” *Nat. Phys.* **11**, 531–538 (2015).
- ⁹J. Nagler, A. Levina, and M. Timme, “Impact of single links in competitive percolation,” *Nat. Phys.* **7**, 265–270 (2011).
- ¹⁰Y. Kuramoto, *Chemical oscillations, waves, and turbulence* (Springer-Verlag, 1984).
- ¹¹D. J. Watts, *Small Worlds* (Princeton University Press, 1999).

- ¹²H. Hong, M. Y. Choi, and B. J. Kim, “Synchronization on small-world networks,” *Phys. Rev. E* **65**, 026139 (2002).
- ¹³T. Ichinomiya, “Frequency synchronization in a random oscillator network,” *Phys. Rev. E* **70**, 026116 (2004).
- ¹⁴J. G. Restrepo, E. Ott, and B. R. Hunt, “The emergence of coherence in complex networks of heterogeneous dynamical systems,” *Phys. Rev. Lett.* **96**, 254103 (2006).
- ¹⁵J. Gómez-Gardeñes, S. Gómez, A. Arenas, and Y. Moreno, “Explosive synchronization transitions in scale-free networks,” *Phys. Rev. Lett.* **106**, 128701 (2011).
- ¹⁶P. Ji, T. K. DM. Peron, P. J. Menck, F. A. Rodrigues, and J. Kurths, “Cluster explosive synchronization in complex networks,” *Phys. Rev. Lett.* **110**, 218701 (2013).
- ¹⁷A. E. Motter, C. Zhou, and J. Kurths, “Enhancing complex-network synchronization,” *Europhys. Lett.* **69**, 334–340 (2005).
- ¹⁸L. Donetti, P. I. Hurtado, and M. A. Muñoz, “Entangled networks, synchronization, and optimal network topology,” *Phys. Rev. Lett.* **95**, 188701 (2005).
- ¹⁹T. Nishikawa and A. E. Motter, “Synchronization is optimal in non-diagonalizable networks,” *Phys. Rev. E* **73**, 065106(R) (2006).
- ²⁰T. Nishikawa and A. E. Motter, “Maximum performance at minimum cost in network synchronization,” *Physica D* **224**, 77–89 (2006).
- ²¹B. Wang, T. Zhou, Z. L. Xiu, and B. J. Kim, “Optimal synchronizability of networks,” *Eur. Phys. J. B* **60**, 89–95 (2007).
- ²²M. Brede, “Optimal synchronization in space,” *Phys. Rev. E* **81**, 025202 (2010).
- ²³Q. Xinyun, W. Lifu, G. Yuan, and W. Yaping, “The optimal synchronizability of a class network,” in *25th Chinese Control and Decision Conference*, pp. 3414–3418 (2013).
- ²⁴Y. Tang, F. Qian, H. Gao, J. Kurths, “Synchronization in complex networks and its application—a survey of recent advances and challenges,” *Annu. Rev. Control* **38**, 184–198 (2014).

- ²⁵L. M. Pecora and T. L. Carroll, “Synchronization of chaotic systems,” *Chaos* **25**, 097611 (2015).
- ²⁶A. Pikovsky and M. Rosenblum, “Dynamics of globally coupled oscillators: Progress and perspectives,” *Chaos* **25**, 097616 (2015).
- ²⁷C. Zhou and J. Kurths, “Hierarchical synchronization in complex networks with heterogeneous degrees,” *Chaos* **16**, 015104 (2006).
- ²⁸T. Dahms, J. Lehnert, and E. Schöll, “Cluster and group synchronization in delay-coupled networks,” *Phys. Rev. E* **86**, 016202 (2012).
- ²⁹L. M. Pecora, F. Sorrentino, A. M. Hagerstrom, T. E. Murphy, and R. Roy, “Cluster synchronization and isolated desynchronization in complex networks with symmetries,” *Nat. Commun.* **5**, 4079 (2014).
- ³⁰A. Bergner, M. Frasca, G. Sciuto, A. Buscarino, E. J. Ngamga, L. Fortuna, and J. Kurths, “Remote synchronization in star networks,” *Phys. Rev. E* **85**, 026208 (2012).
- ³¹V. Nicosia, M. Valencia, M. Chavez, A. Díaz-Guilera, and V. Latora, “Remote synchronization reveals network symmetries and functional modules,” *Phys. Rev. Lett.* **110**, 174102 (2013).
- ³²L. V. Gambuzza, A. Cardillo, A. Fiasconaro, L. Fortuna, J. Gómez-Gardenes, and M. Frasca, “Analysis of remote synchronization in complex networks,” *Chaos* **23**, 043103 (2013).
- ³³I. Fischer, R. Vicente, J. M. Buldú, M. Peil, C. R. Mirasso, M. C. Torrent, and J. García-Ojalvo, “Zero-lag long-range synchronization via dynamical relaying,” *Phys. Rev. Lett.* **97**, 123902 (2006).
- ³⁴Y. Kuramoto and D. Battogtokh, “Existence of coherence and incoherence in nonlocally coupled phase oscillators,” *Nonlinear Phenom. Complex Syst.* **5**, 380 (2002).
- ³⁵D. M. Abrams and S. H. Strogatz, “Chimera states for coupled oscillators,” *Phys. Rev. Lett.* **93**, 174102 (2004).
- ³⁶L. M. Pecora and T. L. Carroll, “Master stability functions for synchronized coupled systems,” *Phys. Rev. Lett.* **80**, 2109–2112 (1998).
- ³⁷F. Chung, *Spectral Graph Theory* (American Mathematical Society, 1997).
- ³⁸A. E. Motter, C. Zhou, and J. Kurths, “Network synchronization, diffusion, and the paradox of heterogeneity,” *Phys. Rev. E* **71**, 016116 (2005).
- ³⁹W. Ren, R. Beard, and E. Atkins, “Information consensus in multivehicle cooperative control,” *IEEE Control Syst. Magazine* **27**, 71–82 (2007).
- ⁴⁰P. Yang, R. Freeman, and K. Lynch, “Multi-agent coordination by decentralized estimation and control,” *IEEE T. Automat. Contr.* **53**, 2480–2496 (2008).
- ⁴¹H. Nakao and A. S. Mikhailov, “Turing patterns in network-organized activator-inhibitor systems,” *Nat. Phys.* **6**, 544–550 (2010).
- ⁴²N. Alon, “Eigenvalues and expanders,” *Combinatorica* **6**, 83–96 (1986).
- ⁴³C. Maas, “Transportation in graphs and the admittance spectrum,” *Discrete Appl. Math.* **16**, 31–49 (1987).
- ⁴⁴A. Lubotzky, R. Phillips, and P. Sarnak, “Ramanujan graphs,” *Combinatorica* **8**, 261–277 (1988).
- ⁴⁵J. Friedman, J. Kahn, and E. Szemerédi, “On the second eigenvalue of random regular graphs,” in *STOC ’89 Proceedings of the twenty-first annual ACM symposium on theory of computing*, D. S. Johnson, ed., pp. 587–598 (ACM, 1989).
- ⁴⁶B. Dionne, M. Golubitsky, and I. Stewart, “Coupled cells with internal symmetry: I. Wreath products,” *Nonlinearity* **9**, 559 (1996).
- ⁴⁷V. N. Belykh, I. V. Belykh, and M. Hasler, “Hierarchy and stability of partially synchronous oscillations of diffusively coupled dynamical systems,” *Phys. Rev. E* **62**, 6332–6345 (2000).
- ⁴⁸A. Pogromsky, G. Santoboni, and H. Nijmeijer, “Partial synchronization: from symmetry towards stability,” *Physica D* **172**, 65–87 (2002).
- ⁴⁹I. Belykh, V. Belykh, K. Nevidin, and M. Hasler, “Persistent clusters in lattices of coupled nonidentical chaotic systems,” *Chaos* **13**, 165–178 (2003).
- ⁵⁰A. Pogromsky, “A partial synchronization theorem,” *Chaos* **18**, 037107 (2008).
- ⁵¹W. Lin, H. Fan, Y. Wang, H. Ying, and X. Wang, “Controlling synchronous patterns in complex networks,” *Phys. Rev. E* **93**, 042209 (2016).
- ⁵²F. Sorrentino, L. M. Pecora, A. M. Hagerstrom, T. E. Murphy, and R. Roy, “Complete characterization of the stability of cluster synchronization in complex dynamical networks,” *Sci. Adv.* **2**, e1501737 (2016).
- ⁵³T. Nishikawa, J. Sun, and A. E. Motter, “Sensitive dependence of optimal network dynamics on network structure,” *Phys. Rev. X* **7**, 041044 (2017).
- ⁵⁴E. N. Lorenz, “Deterministic nonperiodic flow,” *J. Atmos. Sci.* **20**, 130–141 (1963).
- ⁵⁵J. Alexander, J. A. Yorke, Z. You, and I. Kan, “Riddled basins,” *Int. J. Bif. Chaos* **2**, 795–813 (1992).
- ⁵⁶E. Ott, J. C. Sommerer, J. C. Alexander, I. Kan, and J. A. Yorke, “The transition to chaotic attractors with riddled basins,” *Physica D* **76**, 384–410 (1994).
- ⁵⁷M. Golubitsky and I. Stewart, *The Symmetry Perspective: From Equilibrium to Chaos in Phase Space and Physical Space*, Vol. 200 (Springer Science & Business Media, 2003).
- ⁵⁸B. D. MacArthur, R. J. Sánchez-García, and J. W. Anderson, “Symmetry in complex networks,” *Discrete Appl. Math.* **156**, 3525–3531 (2008).